THE JOURNAL OF PHYSICAL CHEMISTRY A

pubs.acs.org/JPCA

Article

Rotational Mode Specificity in the $F^- + CH_3I(v = 0, JK)$ S_N2 and Proton-Transfer Reactions

Paszkál Papp and Gábor Czakó*

Cite This: *J. Phys. Chem. A* 2020, 124, 8943–8948

Read Online

ACCESS | Metrics & More | Article Recommendations

ABSTRACT: Quasiclassical trajectory computations are performed for the $F^- + CH_3I(v = 0, JK) \rightarrow I^- + CH_3F$ (S_N2) and $HF + CH_2I^-$ (proton-transfer) reactions considering initial rotational states characterized by $J = \{0, 2, 4, 6, 8, 12, \text{and } 16\}$ and $K = \{0 \text{ and } J\}$ in the 1−30 kcal/mol collision energy (E_{coll}) range. Tumbling rotation ($K = 0$) counteracts orientation effects, thereby hindering the S_N2 reactivity by about 15% for $J = 16$ in the 1−15 kcal/mol E_{coll} range and has a negligible effect on proton transfer. Spinning about the C−I bond ($K = J$), which is 21 times faster than tumbling, makes the reactions more direct, inhibiting the S_N2 reactivity by 25% in some cases, whereas significantly enhancing the proton-transfer channel by a factor of 2 at $E_{coll} = 15$ kcal/mol due to the fact that the spinning-induced centrifugal force hinders complex formation by breaking H-bonds and activates C−H bond cleavage, thereby promoting proton abstraction on the expense of substitution. At higher E_{coll}, as the reactions become more direct, the rotational effects are diminishing.

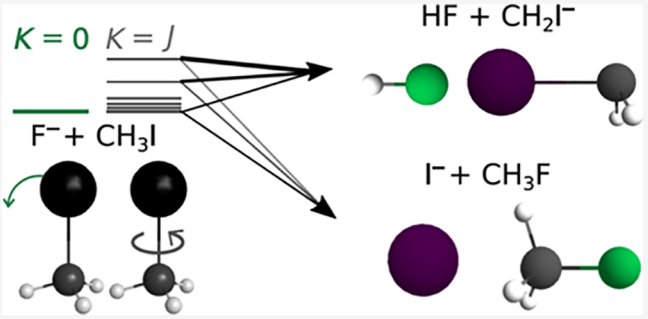

1. INTRODUCTION

Mode-specific excitation of the reactant allows controlling the outcome of a chemical reaction, which has always been a major goal of chemistry. Following many vibrational mode-specific experimental and theoretical studies of polyatomic reaction dynamics,[1−10] the concept of "rotational mode specificity" was introduced in 2014 in the case of the $Cl + CHD_3 \rightarrow HCl + CD_3$ reaction.[11] CHD_3 is a symmetric top, which can be characterized by the total rotational angular momentum quantum number J and its projection K to the body-fixed axis. Different K values, that is, 0, ±1, ..., ±J, correspond to different rotational "modes" (states), such as tumbling and spinning rotations considering the two limiting cases of $K = 0$ and $K = \pm J$, respectively. On the one hand, it has long been well known that the excitation of different vibrational modes, such as stretching, bending, and torsion, may have significantly different effects on chemical reactivity. On the other hand, the rotational mode specific investigations do not have such a long history; nevertheless, several experimental and theoretical studies have recently started to uncover the effect of the initial rotational state on the reactivity of polyatomic reactions.[12−23] Rotational mode specificity was studied for the ($H_2O^+ + H_2/D_2$,[12,13] $H/F/Cl + H_2O$[14,15]), $F/Cl/OH + CH_4$,[16−19] and ($H/Cl/O + CHD_3$,[11,20−22] $F^- + CH_3F/CH_3Cl$[23]) reactions involving asymmetric, spherical, and symmetric top polyatomic reactants, respectively. In the present study, we focus on the reaction of another symmetric top molecule CH_3I with F^-, thus the most relevant previous systems are $H/Cl/O + CHD_3$ and $F^- + CH_3F/CH_3Cl$. The former H-abstraction reactions are enhanced by rotational excitation,[11,22] except $H + CHD_3$, where rotational effects up to $J = 2$ were found to be negligible.[20] For $Cl/O + CHD_3$, significant rotational mode specificity was observed as tumbling and spinning rotations showed substantial and modest enhancement factors, respectively.[11,22] In the case of the $F^- + CH_3F/CH_3Cl$ S_N2 reactions, rotational excitation hinders the reactivity with significant K dependence.[23] Unlike for $Cl/O + CHD_3$,[11,22] for the $F^- + CH_3Cl$ S_N2 reaction tumbling rotation has a less significant effect than spinning, whereas for $F^- + CH_3F$ both rotational modes effectively hinder depending on collision energy as well.[23]

The $F^- + CH_3I$ reaction has recently been investigated by several theoretical and crossed-beam experimental studies.[24−37] In 2017, we reported a high-level full-dimensional analytical ab initio potential energy surface (PES) for the $F^- + CH_3I$ system, allowing efficient dynamics investigations of both the S_N2 and proton-transfer channels.[27] In 2018, our joint theoretical−experimental study showed that symmetric CH

Received: September 3, 2020
Revised: October 1, 2020
Published: October 15, 2020

https://dx.doi.org/10.1021/acs.jpca.0c08043
J. Phys. Chem. A 2020, 124, 8943–8948

stretching excitation is a spectator mode in the S_N2 reaction, whereas it enhances the proton-transfer channel.[32] Later, we reported detailed vibrational mode specific simulations for the $F^- + CH_3I$ S_N2 and proton-transfer reactions,[33] which were followed by additional crossed-beam measurements by the Wester group.[35,36] Rotational mode specific investigations have not been reported for the title reaction before; thus, the present study aims to be the first step toward this direction. Moreover, our previous study[23] on the *JK*-specific dynamics computations for the $F^- + CH_3F/CH_3Cl$ reactions considered the S_N2 channel only, whereas the present work reports rotational mode specific simulations for both the S_N2 and proton-transfer channels of the $F^- + CH_3I$ reaction.

2. COMPUTATIONAL DETAILS

Reaction dynamics simulations are performed for the $F^- + CH_3I(v = 0, JK)$ reaction using the quasi-classical trajectory method and a high-level full-dimensional analytical ab initio PES taken from ref 27. Standard normal mode sampling[38] is employed to prepare the initial quasi-classical ground vibrational state ($v = 0$), and the *JK* rotational states are set using the procedure described in detail in ref 23. In brief, the length of the classical angular momentum vector of the CH_3I molecule is set to $[J(J + 1)]^{1/2}$ in atomic units and its direction is randomly sampled while keeping its projection to the *a* principal axis (C−I bond assuming C_{3v} symmetry) fixed at the value of *K*. The interested reader can check eqs 1−6 of ref 23 to find the mathematical formulas used in the present implementation. Trajectories are run at collision energies (E_{coll}) of 1, 4, 7, 10, 15, 20, and 30 kcal/mol. The initial distance of the reactants is $(x^2 + b^2)^{1/2}$, where $x = 40$ bohr ($E_{coll} = 1$ kcal/mol), 30 bohr ($E_{coll} = 4$ kcal/mol), and 20 bohr ($E_{coll} \geq 7$ kcal/mol), the orientation of CH_3I is randomly sampled, and the impact parameter (b) is scanned from 0 to b_{max} with a step size of 1 bohr. b_{max} values of 30, 20, 18, 15, 14, 12, and 10 bohr are used at the above collision energies, respectively. For each *JK* initial state, 1000 (5000) trajectories are computed at each b at E_{coll} of 1, 4, 7, and 10 kcal/mol, (15, 20, and 30 kcal/mol). In this study, we consider *J* values of 0, 2, 4, 6, 8, 12, and 16 with $K = 0$ and *J*. Trajectories are propagated using a time step of 0.0726 fs until the maximum of the internuclear distances becomes one bohr larger than the initial one. Cross sections are obtained using a b-weighted numerical integration of the reaction probabilities over b from 0 to b_{max} without applying any zero-point energy constraint.

3. RESULTS AND DISCUSSION

The pathways of the S_N2 and proton-transfer channels of the $F^- + CH_3I$ reaction leading to $I^- + CH_3F$ and $HF + CH_2I^-$, respectively, are shown in Figure 1. The Walden-inversion S_N2 channel is highly exothermic and goes through several submerged minima and transition states. The lowest-energy configuration of the entrance channel is a halogen-bonded front-side complex ($H_3CI\cdots F^-$), which steers the reactants away from the reactive configurations, thereby making the S_N2 reaction indirect.[29,39] There are two different S_N2 retention pathways via DITS (double inversion) and FSTS (front-side attack), as can be seen in Figure 1, but these mechanisms have less relevance to the present study.[27,40] The proton-transfer channel is endothermic with several stationary points between the reactant and product asymptotes. The tumbling ($K = 0$) and spinning ($K = J$) rotational modes and the initial rotational

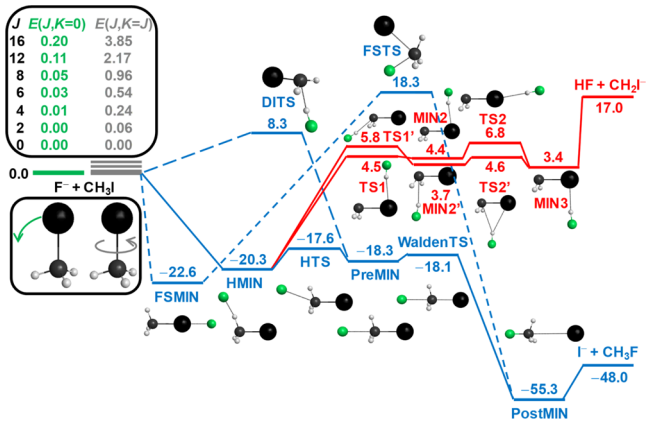

Figure 1. Schematic PES[27] of the $F^- + CH_3I$ reaction showing the rigid-rotor energies (kcal/mol) of the reactant corresponding to selected *JK* rotational states considered in the present study and the classical relative energies (kcal/mol) of the stationary points along the S_N2 (blue) and proton-transfer (red) channels.

states of CH_3I considered in the present study are also shown in Figure 1. The *A* and *B* rotational constants of the prolate-type CH_3I molecule are 5.24 and 0.25 cm^{-1}, that is, 0.0150 and 0.0007 kcal/mol, respectively, which result in very low tumbling rotational energy levels such as $E(J, K = 0) = BJ(J + 1)$ and relatively higher spinning levels with energies of $E(J, K = J) = AJ^2 + BJ$. Thus, as seen in Figure 1, the $K = 0$ levels up to $J = 16$ spans an energy range from 0.00 to 0.20 kcal/mol, whereas the $K = J$ levels go up to 3.85 kcal/mol for $J = 0-16$.

The *JK*-dependent excitation functions (cross sections as a function of E_{coll}) for the S_N2 and proton-transfer channels are shown in Figures 2 and 3, respectively. The S_N2 cross sections are large and sharply decrease with increasing E_{coll}, as expected in the case of a barrier-less exothermic reaction. Rotational excitation hinders the S_N2 channel especially at low collision energies, as seen in Figure 2. The inhibition is modest for tumbling rotation, that is, less than 5% for *J* up to 8 and about 10−15% for $J = 12-16$, whereas it is more significant in the case of a spinning reactant, that is, around 5−10% for $J = 4$ and can be 25% for $J = 16$ depending on E_{coll}. These rotational inhibition effects are very similar to those previously found for the $F^- + CH_3Cl$ S_N2 reaction.[23] The picture is quite different for the proton-transfer (proton-abstraction) channel of the $F^- + CH_3I$ reaction, as shown in Figure 3. The proton-transfer cross sections increase with collision energy and significant rotational enhancement is found upon spinning excitation, whereas tumbling rotation has a negligible effect (few % inhibition, which is comparable with statistical uncertainty) on proton abstraction. At $E_{coll} = 15$ kcal/mol, the $K = J$ rotational excitations increase the cross sections by factors of 1.1 and 2.2 for $J = 8$ and 16, respectively, and the enhancement factors decrease with increasing E_{coll}, as shown in Figure 3.

To get deeper insights into the rotational mode specific dynamics of the title reaction, opacity functions (reaction probabilities as a function of b) as well as scattering angle, initial attack angle, and product relative translational energy distributions are also computed at $E_{coll} = 15$ kcal/mol and presented in Figures 4 and 5 for the S_N2 and proton-transfer channels, respectively. The initial attack angle is defined as the angle between the center of the mass velocity vector of CH_3I and the CI vector at the beginning of the trajectories. Attack

https://dx.doi.org/10.1021/acs.jpca.0c08043
J. Phys. Chem. A 2020, 124, 8943−8948

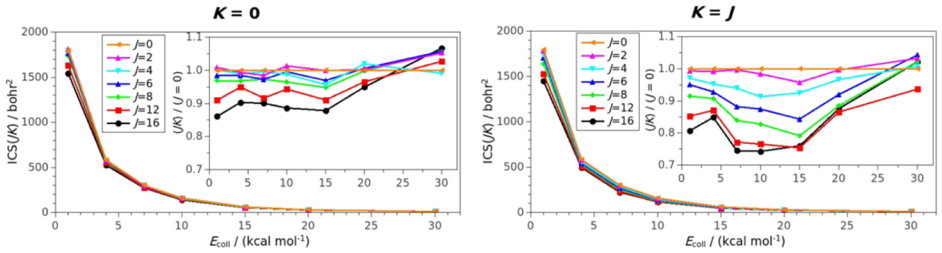

Figure 2. *JK* dependence of the cross sections and their ratios for the $F^- + CH_3I(v = 0, JK) \rightarrow I^- + CH_3F$ S_N2 reaction as a function of collision energy.

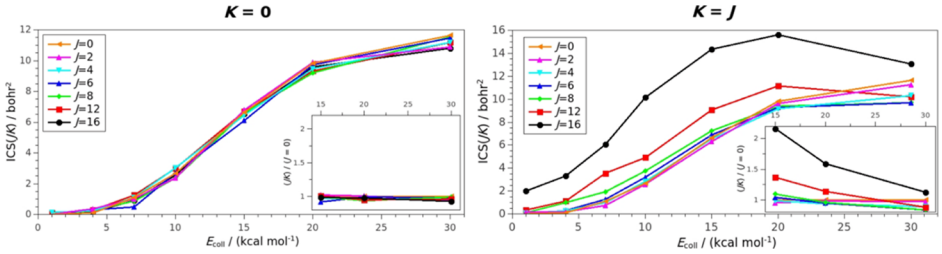

Figure 3. *JK* dependence of the cross sections and their ratios for the $F^- + CH_3I(v = 0, JK) \rightarrow HF + CH_2I^-$ proton-transfer reaction as a function of collision energy.

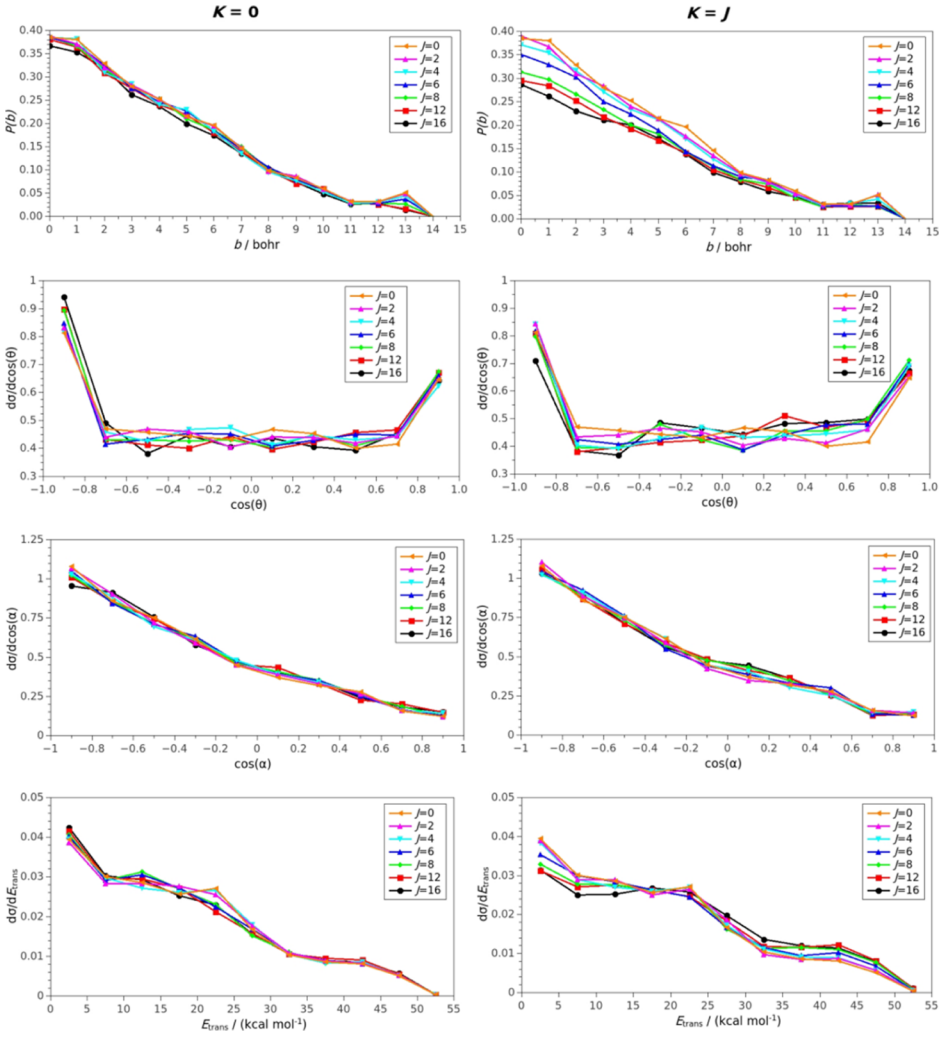

Figure 4. *JK* dependence of the opacity functions $(P(b))$ as well as of the normalized scattering angle (θ), initial attack angle (α), and product relative translational energy (E_{trans}) distributions at a collision energy of 15 kcal/mol for the $F^- + CH_3I(v = 0, JK) \rightarrow I^- + CH_3F$ S_N2 reaction.

https://dx.doi.org/10.1021/acs.jpca.0c08043
J. Phys. Chem. A 2020, 124, 8943−8948

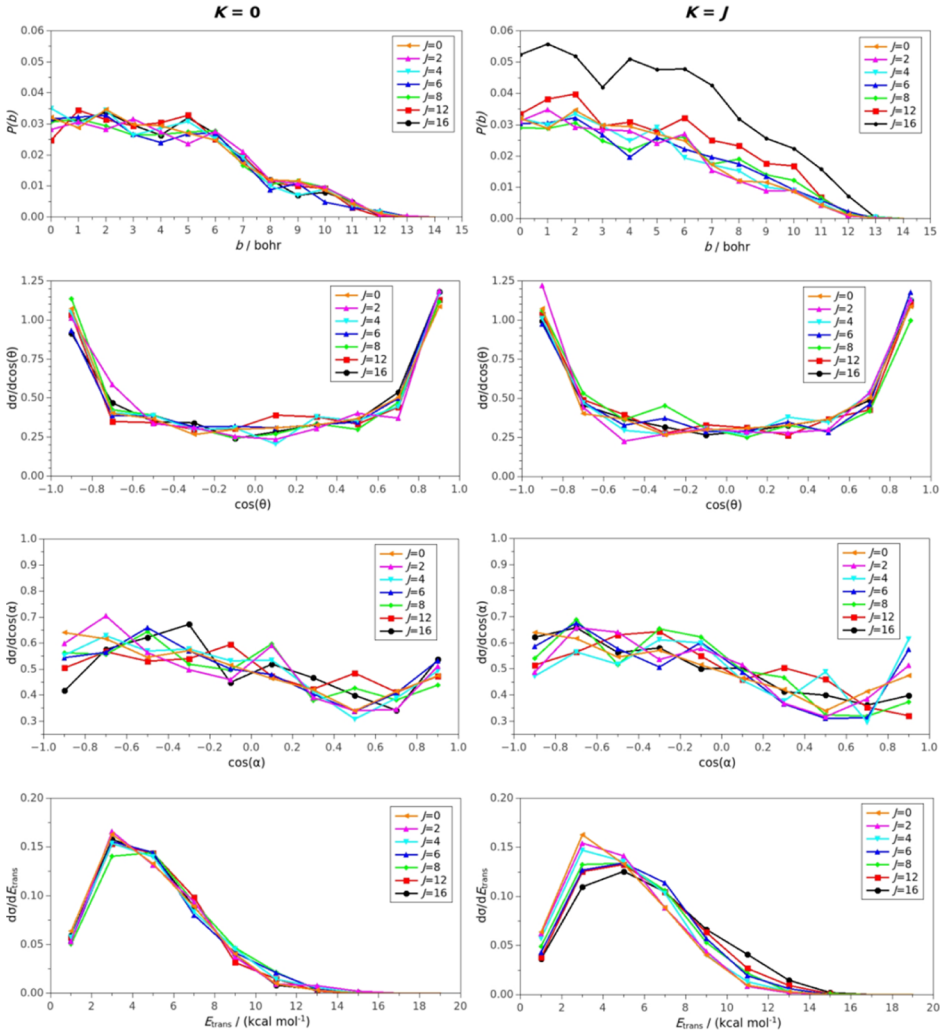

Figure 5. *JK* dependence of the opacity functions ($P(b)$) as well as of the normalized scattering angle (θ), initial attack angle (α), and product relative translational energy (E_{trans}) distributions at a collision energy of 15 kcal/mol for the $F^- + CH_3I(v = 0, JK) \rightarrow HF + CH_2I^-$ proton-transfer reaction.

angle 0° corresponds to the approach of the iodine side, whereas 180° describes the methyl-attack pathways.

For the $J = 0$ initial state, the S_N2 reaction probability is about 39% at $b = 0$, decreases almost linearly with increasing b and vanishes at $b = 14$, as shown in Figure 4. On the one hand, tumbling rotational excitations ($K = 0$) have a modest effect on the opacity functions, which slightly decrease the reaction probabilities without affecting the shape of the opacity curves. On the other hand, spinning rotation ($K = J$) significantly decreases the reaction probabilities especially at small b values. For example, at $b = 0$, the $J = 8$ and 16 reaction probabilities are only 31 and 29% for $K = J$, respectively, whereas the corresponding $K = 0$ values are 39 and 37%. The scattering angle distributions are backward−forward symmetric, isotropic in the $\cos(\theta)$ range from −0.8 and +0.8 (indicating significant complex-forming indirect trajectories), and peak both in the backward (direct rebound) and forward (direct stripping) directions. The initial attack angle distributions clearly favor the backside (methyl-side) attack and the reactivity decreases as the attack angle goes from 180 to 0° as expected for an S_N2 reaction. However, it is important to note that the reactivity corresponding to the 0−90° (front-side) attack angle range is not negligible (about 25% of the total reactivity), indicating again nontraditional indirect dynamics. Significant *JK* dependence is not found for the scattering and attack angle distributions, except for some decrease of the backward scattering upon spinning excitations, in accordance with the decreasing S_N2 reaction probabilities at small impact parameters. Product relative translational energy distributions are broad and rather cold, peaking at the lowest energies supporting the indirect nature of the S_N2 reaction. Tumbling rotation does not affect these distributions significantly; however, spinning excitations clearly shift the distributions toward higher product relative translational energies making the reaction more direct. A similar conclusion about the indirect−direct nature was previously found for the F^- + CH_3Cl S_N2 reaction based on the analysis of the integration time.[23]

The proton-transfer reaction opacity functions are nearly constant in the $b = 0$−6 bohr range and then decrease reaching b_{max} values around 13 bohr, as shown in Figure 5. Tumbling rotational excitation has a negligible effect on the reaction probabilities, whereas spinning excitation significantly increases the reactivity especially at large b values, although the b_{max} value is not affected. Scattering angle distributions are backward−forward symmetric without significant *JK*-depend-

https://dx.doi.org/10.1021/acs.jpca.0c08043
J. Phys. Chem. A 2020, 124, 8943−8948

ence, similar to the S_N2 channel. Attack angle distributions are rather isotropic with some preference for the methyl-side attack, and again, the rotational dependence is within the level of statistical uncertainty. Product relative translational energy distributions range between 0 and 15 kcal/mol (Figure 5), which is significantly colder than those of the S_N2 channel spanning the 0−50 kcal/mol energy range (Figure 4). This is expected, because the S_N2 reaction is highly exothermic, whereas proton-transfer is endothermic. The $J = 0$ proton-transfer translational energy distribution peaks at about 3 kcal/mol without any significant J dependence in the case of $K = 0$. However, for $K = J$ the peak shifts toward 5 kcal/mol and the distributions become hotter as J increases, indicating that the proton transfer becomes more direct upon excitation of the spinning rotation.

On the basis of the above-described results, we propose the following explanation for the rotational mode specificity in the title reaction. Considering the magnitudes of the rotational constants of the CH_3I molecule ($A = 5.24$ cm^{-1} and $B = 0.25$ cm^{-1}), one can see that the spinning rotation about the a principal axis (C−I bond) is $A/B = I_b/I_a = 21$ times faster than tumbling rotation corresponding to the same J because the rotational constants are inversely proportional to the components of the principal moment of inertia (I_a and I_b), and the angular velocity is $\mathbf{I}^{-1}\mathbf{J}$. The large angular velocity in the case of the spinning rotation about the C−I axis induces a substantial centrifugal force which facilitates C−H bond cleavage, thereby enhancing the proton-abstraction channel, on the expense of substitution. Furthermore, the centrifugal force hinders long-lived complex formation by breaking H-bonds; thus, making the S_N2 process more direct and less reactive in the case of spinning rotation. At low collision energies, the H-bond breaking effect hinders the S_N2 channel, then, as E_{coll} increases, the enhanced break of the C−H bond further suppresses the substitution reaction while the proton abstraction is activated. Tumbling rotation also slightly hinders the S_N2 reaction by counteracting the orientation effects, but this effect is not substantial because of the small angular velocity caused by the large I_b value. Rotational effects diminish at high collision energies as the reaction becomes more direct and complex formations as well as orientation do not play key roles in the dynamics.

4. SUMMARY AND CONCLUSIONS

We have performed rotational mode specific quasi-classical simulations for the $F^- + CH_3I$ reaction considering several different tumbling ($K = 0$) and spinning ($K = J$) rotational states up to $J = 16$. The reaction dynamics computations utilize our recently developed high-level analytical ab initio PES,[27] which describes both the S_N2 and proton-transfer channels of the title reaction. Rotational excitations hinder the S_N2 reaction more and more significantly with increasing J, especially for spinning rotation and low or modest collision energies. The proton-transfer channel is virtually not affected upon tumbling excitations however substantially enhanced by spinning rotation. Scattering and initial attack angle distributions do not show significant JK-dependence, whereas product relative translation energy distributions become hotter and hotter as J increases with $K = J$, showing that spinning excitations make the reactions more direct. The present findings for the S_N2 channel are similar to those of our previous study on the $F^- + CH_3Cl$ S_N2 reaction, where we suggested that tumbling and spinning rotations may hinder orientation and complex formation, respectively, thereby suppressing the substitution reactivity.[23] Here, for the first time, we study the proton-transfer channel as well, which helps to complete the picture. We propose that the centrifugal force induced by fast spinning rotation about the C−I bond axis facilitate C−H bond breaking, thereby enhancing the proton-abstraction channel, on the expense of the S_N2 reactivity. Thus, spinning excitations hinder the S_N2 channel because of breaking H-bonds (low E_{coll}) and C−H bond (modest E_{coll}, where the abstraction channel opens). The situation of the mainly indirect $F^- + CH_3I$ reaction is quite different from the case of the previously studied $Cl/O + CHD_3$ direct H-abstraction reactions, where tumbling rotation enhanced the reactivity because of enlarging the reactive attack angle range, whereas spinning excitations had less significant enhancement effects.[11,22] We hope that following the JK-specific measurements for the $Cl + CHD_3$ reaction,[11] rotational mode specific experiments will be carried out for the title reaction in the near future.

AUTHOR INFORMATION

Corresponding Author

Gábor Czakó − *MTA-SZTE Lendület Computational Reaction Dynamics Research Group, Interdisciplinary Excellence Centre and Department of Physical Chemistry and Materials Science, Institute of Chemistry, University of Szeged, Szeged H-6720, Hungary;* orcid.org/0000-0001-5136-4777; Email: gczako@chem.u-szeged.hu

Author

Paszkál Papp − *MTA-SZTE Lendület Computational Reaction Dynamics Research Group, Interdisciplinary Excellence Centre and Department of Physical Chemistry and Materials Science, Institute of Chemistry, University of Szeged, Szeged H-6720, Hungary*

Complete contact information is available at: https://pubs.acs.org/10.1021/acs.jpca.0c08043

Notes

The authors declare no competing financial interest.

ACKNOWLEDGMENTS

We thank the National Research, Development and Innovation Office—NKFIH, K-125317, the Ministry of Human Capacities, Hungary grant 20391-3/2018/FEKUSTRAT, and the Momentum (Lendület) Program of the Hungarian Academy of Sciences for financial support.

REFERENCES

(1) Schatz, G. C.; Colton, M. C.; Grant, J. L. A Quasiclassical Trajectory Study of the State-to-State Dynamics of $H + H_2O \rightarrow OH + H_2$. *J. Phys. Chem.* **1984**, *88*, 2971−2977.

(2) Sinha, A.; Hsiao, M. C.; Crim, F. F. Bond-Selected Bimolecular Chemistry: $H + HOD(4\nu_{OH}) \rightarrow OD + H_2$. *J. Chem. Phys.* **1990**, *92*, 6333−6335.

(3) Bronikowski, M. J.; Simpson, W. R.; Girard, B.; Zare, R. N. Bond-Specific Chemistry: OD:OH Product Ratios for the Reactions H + HOD(100) and H + HOD(001). *J. Chem. Phys.* **1991**, *95*, 8647−8648.

(4) Zhang, D. H.; Light, J. C. Mode Specificity in the H + HOD Reaction. Full-Dimensional Quantum Study. *J. Chem. Soc., Faraday Trans.* **1997**, *93*, 691−697.

(5) Yoon, S.; Henton, S.; Zivkovic, A. N.; Crim, F. F. The Relative Reactivity of the Stretch−Bend Combination Vibrations of CH_4 in

the $Cl(^2P_{3/2})$ + CH_4 Reaction. *J. Chem. Phys.* **2002**, *116*, 10744−10752.
(6) Yan, S.; Wu, Y.-T.; Zhang, B.; Yue, X.-F.; Liu, K. Do Vibrational Excitations of CHD_3 Preferentially Promote Reactivity Toward the Chlorine Atom? *Science* **2007**, *316*, 1723−1726.
(7) Czakó, G.; Bowman, J. M. Dynamics of the Reaction of Methane with Chlorine Atom on an Accurate Potential Energy Surface. *Science* **2011**, *334*, 343−346.
(8) Liu, R.; Yang, M.; Czakó, G.; Bowman, J. M.; Li, J.; Guo, H. Mode Selectivity for a "Central" Barrier Reaction: Eight-Dimensional Quantum Studies of the $O(^3P)$ + CH_4 → OH + CH_3 Reaction on an ab Initio Potential Energy Surface. *J. Phys. Chem. Lett.* **2012**, *3*, 3776−3780.
(9) Espinosa-García, J.; Quasiclassical, J. Trajectory Calculations Analyzing the Role of Vibrational and Translational Energy in the F + CH_2D_2 Reaction. *J. Chem. Phys.* **2009**, *130*, 054305.
(10) Jiang, B.; Guo, H. Control of Mode/Bond Selectivity and Product Energy Disposal by the Transition State: X + H_2O (X = H, F, $O(^3P)$, and Cl) Reactions. *J. Am. Chem. Soc.* **2013**, *135*, 15251−15256.
(11) Liu, R.; Wang, F.; Jiang, B.; Czakó, G.; Yang, M.; Liu, K.; Guo, H. Rotational Mode Specificity in the Cl + CHD_3 → HCl + CD_3 Reaction. *J. Chem. Phys.* **2014**, *141*, 074310.
(12) Xu, Y.; Xiong, B.; Chang, Y. C.; Ng, C. Y. Communication: Rovibrationally Selected Absolute Total Cross Sections for the Reaction $H_2O^+(X^2B_1; v_1^+v_2^+v_3^+ = 000; N^+_{Ka+Kc+})$ + D_2: Observation of the Rotational Enhancement Effect. *J. Chem. Phys.* **2012**, *137*, 241101.
(13) Li, A.; Li, Y.; Guo, H.; Lau, K.-C.; Xu, Y.; Xiong, B.; Chang, Y.-C.; Ng, C. Y. Communication: The Origin of Rotational Enhancement Effect for the Reaction of H_2O^+ + H_2 (D_2). *J. Chem. Phys.* **2014**, *140*, 011102.
(14) Jiang, B.; Li, J.; Guo, H. Effects of Reactant Rotational Excitation on Reactivity: Perspectives from the Sudden Limit. *J. Chem. Phys.* **2014**, *140*, 034112.
(15) Song, H.; Guo, H. Vibrational and Rotational Mode Specificity in the Cl + H_2O → HCl + OH Reaction: A Quantum Dynamical Study. *J. Phys. Chem. A* **2015**, *119*, 6188−6194.
(16) Cheng, Y.; Pan, H.; Wang, F.; Liu, K. On the Signal Depletion Induced by Stretching Excitation of Methane in the Reaction with the F Atom. *Phys. Chem. Chem. Phys.* **2014**, *16*, 444−452.
(17) Meng, F.; Yan, W.; Wang, D. Quantum Dynamics Study of the Cl + CH_4 → HCl + CH_3 Reaction: Reactive Resonance, Vibrational Excitation Reactivity, and Rate Constants. *Phys. Chem. Chem. Phys.* **2012**, *14*, 13656−13662.
(18) Pan, H.; Cheng, Y.; Liu, K. Rotational Mode Specificity in Cl + $CH_4(v_3=1,|jNl\rangle)$: Role of Reactant's Vibrational Angular Momentum. *J. Phys. Chem. A* **2016**, *120*, 4799−4804.
(19) Song, H.; Li, J.; Jiang, B.; Yang, M.; Lu, Y.; Guo, H. Effects of Reactant Rotation on the Dynamics of the OH + CH_4 → H_2O + CH_3 Reaction: A Six-Dimensional Study. *J. Chem. Phys.* **2014**, *140*, 084307.
(20) Zhang, Z.; Zhang, D. H. Effects of Reagent Rotational Excitation on the H + CHD_3 → H_2 + CD_3 Reaction: A Seven Dimensional Time-Dependent Wave Packet Study. *J. Chem. Phys.* **2014**, *141*, 144309.
(21) Wang, F.; Pan, H.; Liu, K. Imaging the Effects of Reactant Rotations on the Dynamics of the Cl + $CHD_3(v_1 = 1, |J,K\rangle)$ Reaction. *J. Phys. Chem. A* **2015**, *119*, 11983−11988.
(22) Czakó, G. Quasiclassical Trajectory Study of the Rotational Mode Specificity in the $O(^3P)$ + $CHD_3(v_1 = 0,1, JK)$ → OH + CD_3 Reactions. *J. Phys. Chem. A* **2014**, *118*, 11683−11687.
(23) Szabó, I.; Czakó, G. Rotational Mode Specificity in the F^- + CH_3Y [Y = F and Cl] S_N2 reactions. *J. Phys. Chem. A* **2015**, *119*, 12231−12237.
(24) Zhang, J.; Mikosch, J.; Trippel, S.; Otto, R.; Weidemüller, M.; Wester, R.; Hase, W. L. F^- + CH_3I → FCH_3 + I^- Reaction Dynamics. Nontraditonal Atomistic Mechanisms and Formation of a Hydrogen-Bonded Complex. *J. Phys. Chem. Lett.* **2010**, *1*, 2747−2752.
(25) Mikosch, J.; Zhang, J.; Trippel, S.; Eichhorn, C.; Otto, R.; Sun, R.; de Jong, W. A.; Weidemüller, M.; Hase, W. L.; Wester, R. Indirect Dynamics in a Highly Exoergic Substitution Reaction. *J. Am. Chem. Soc.* **2013**, *135*, 4250−4259.
(26) Zhang, J.; Xie, J.; Hase, W. L. Dynamics of the F^- + CH_3I → HF + CH_2I^- Proton Transfer Reaction. *J. Phys. Chem. A* **2015**, *119*, 12517−12525.
(27) Olasz, B.; Szabó, I.; Czakó, G. High-Level ab Initio Potential Energy Surface and Dynamics of the F^- + CH_3I S_N2 and Proton-Transfer Reactions. *Chem. Sci.* **2017**, *8*, 3164−3170.
(28) Ma, Y.-T.; Ma, X.; Li, A.; Guo, H.; Yang, L.; Zhang, J.; Hase, W. L. Potential Energy Surface Stationary Points and Dynamics of the F^- + CH_3I Double Inversion Mechanism. *Phys. Chem. Chem. Phys.* **2017**, *19*, 20127−20136.
(29) Szabó, I.; Olasz, B.; Czakó, G. Deciphering Front-Side Complex Formation in S_N2 Reactions via Dynamics Mapping. *J. Phys. Chem. Lett.* **2017**, *8*, 2917−2923.
(30) Győri, T.; Olasz, B.; Paragi, G.; Czakó, G. Effects of the Level of Electronic Structure Theory on the Dynamics of the F^- + CH_3I Reaction. *J. Phys. Chem. A* **2018**, *122*, 3353−3364.
(31) Carrascosa, E.; Michaelsen, T.; Stei, M.; Bastian, B.; Meyer, J.; Mikosch, J.; Wester, R. Imaging Proton Transfer and Dihalide Formation Pathways in Reactions of F^- + CH_3I. *J. Phys. Chem. A* **2016**, *120*, 4711−4719.
(32) Stei, M.; Carrascosa, E.; Dörfler, A.; Meyer, J.; Olasz, B.; Czakó, G.; Li, A.; Guo, H.; Wester, R. Stretching Vibration Is Spectator in Nucleophilic Substitution. *Sci. Adv.* **2018**, *4*, No. eaas9544.
(33) Olasz, B.; Czakó, G. Mode-Specific Quasiclassical Dynamics of the F^- + CH_3I S_N2 and Proton-Transfer Reactions. *J. Phys. Chem. A* **2018**, *122*, 8143−8151.
(34) Olasz, B.; Czakó, G. Uncovering the Role of the Stationary Points in the Dynamics of the F^- + CH_3I Reaction. *Phys. Chem. Chem. Phys.* **2019**, *21*, 1578−1586.
(35) Michaelsen, T.; Bastian, B.; Strübin, P.; Meyer, J.; Wester, R. Proton Transfer Dynamics Modified by CH-Stretching Excitation. *Phys. Chem. Chem. Phys.* **2020**, *22*, 12382−12388.
(36) Michaelsen, T.; Bastian, B.; Ayasli, A.; Strübin, P.; Meyer, J.; Wester, R. Influence of Vibrational Excitation on the Reaction of F^- with CH_3I: Spectator Mode Behavior, Enhancement, and Suppression. *J. Phys. Chem. Lett.* **2020**, *11*, 4331−4336.
(37) Liu, P.; Zhang, J.; Wang, D. Multi-Level Quantum Mechanics Theories and Molecular Mechanics Study of the Double-Inversion Mechanism of the F^- + CH_3I Reaction in Aqueous Solution. *Phys. Chem. Chem. Phys.* **2017**, *19*, 14358−14365.
(38) Hase, W. L. *Encyclopedia of Computational Chemistry*; Wiley: New York, 1998; p 399−407.
(39) Stei, M.; Carrascosa, E.; Kainz, M. A.; Kelkar, A. H.; Meyer, J.; Szabó, I.; Czakó, G.; Wester, R. Influence of the Leaving Group on the Dynamics of a Gas-Phase S_N2 Reaction. *Nat. Chem.* **2016**, *8*, 151−156.
(40) Szabó, I.; Czakó, G. Revealing a Double-Inversion Mechanism for the F^- + CH_3Cl S_N2 Reaction. *Nat. Commun.* **2015**, *6*, 5972.

https://dx.doi.org/10.1021/acs.jpca.0c08043
J. Phys. Chem. A 2020, 124, 8943−8948